Original Article

DOI: 10.5582/bst.2014.01035

Fabrication and bioactivity evaluation of porous anodised TiO_2 films *in vitro*

Fei Teng[1,*], Juanjuan Li[1,2,*], Yanyun Wu[1], Haohua Chen[1], Qi Zhang[1], Hu Wang[1], Guomin Ou[1,]**

[1] *West China School of Stomatology, Sichuan University, Chengdu, Sichuan, China;*
[2] *Center of Dental Implantation, the Third Affiliated Hospital of Xinxiang Medical University, Henan, China.*

Summary **This study aims to find an optimal method for modifying the neck of dental implants for gingival attachment through *in vitro* investigations of the biological features of various anodised TiO_2 films. The titanium sheets were divided into four groups: a control group and three test groups classified according to the anodisation voltage (Group 150 V, Group 180 V or Group 200 V).The surface microstructure and crystal structure were observed using scanning electron microscopy and X-ray diffraction. The protein adsorption ability, antibacterial activity and cell adhesion ability were tested to examine the biological properties of the materials *in vitro*. Microscopic grooves were observed in the control group, whereas the test groups contained numerous pores. Group 180 V and Group 200 V showed higher protein adsorption ability ($p < 0.05$), whereas Group 150 V and Group 180 V exhibited better antibacterial activity ($p < 0.05$). Higher cell concentrations of L929 were observed in Group 180V and Group 200 V than in the other two groups ($p < 0.05$), which indicated that the TiO_2 films formed at 180 V promote protein adsorption and enhance fibroblast growth while inhibiting bacterial adhesion. These results indicate that anodisation positively affects the formation of a biological seal in the neck region of dental implants.**

Keywords: Anodic oxidation, TiO_2 film, biomaterials, surfaces, *in vitro* bioactivity

1. Introduction

Titanium and its alloys are used for dental implants because of their low toxicity, low corrosion rate, favourable mechanical properties and excellent biocompatibility (*1*). However, bone loss often occurs in the alveolar crest surrounding the dental implants, and a stable biochemical connection between the neck part of the implant and gingival tissue is difficult to achieve. These findings can be attributed to the lack of natural biological width and functionally oriented fibre (*2-4*).

The formation of a firm soft tissue barrier around the dental implant neck is considered important to prevent bacterial invasion (*5*). To control plaque formation around the neck, most current designs for this region are mechanically machined to achieve a smooth surface, which facilitates the proliferation of epithelial cells. However, unlike the orientation perpendicular to the natural teeth surface, the orientation of the collagen fibres in the connective tissue was found to be parallel to the implant surface (*6,7*), which may cause epithelial down growth after the implants have been inserted (*8*).

To resolve these issues, an on-going goal in bioengineering is to modify titanium implant surfaces and establish the bionic attachment of peri-implant soft tissues in the neck region. A coating for the neck that can help reduce plaque accumulation and form a good seal would be desirable (*9,10*). Several studies have revealed that the micro-roughening of surfaces not only inhibits the formation of plaque but also facilitates the growth of epithelial cells and fibroblasts (*11*). The anchor-shaped structure formed by cellular processes and that extends into the pores on the material

*These authors contributed equally to this works.
***Address correspondence to:*
Dr. Guomin Ou, Department of Implantology, West China School of Stomatology, Sichuan University. NO.14, 3rd Section of Ren Min Nan Rd. Chengdu, Sichuan 610041, China.
E-mail: guominou66@yahoo.com

effectively inhibits the migration of the junctional epithelium to the root square (*12,13*).

To obtain this type of micro-roughened surface, several techniques, such as anodic oxidation, plasma spraying, ion planting, sol-gel, sputtering and chemical vapour deposition (*14,15*), have been used to produce oxide films on titanium and its alloys. Among these methods, anodic oxidation treatment, which can be readily applied to implants with irregular and complex surface geometries (*16*), has become more attractive in recent years. Moreover, a porous TiO_2 layer can be obtained at low temperatures, and the morphology and crystallinity of the oxides can be well controlled by changing the voltage, current density and electrolyte (*17-19*).

In this study, anodic oxidation was adopted to form a porous film with different pore sizes on titanium surfaces. The aim of this study was to create a desirable interface that not only enhances the connection between the host and implant but also inhibits microbial adhesion.

2. Materials and Methods

2.1. *Sample preparation*

Commercially pure titanium of ASTM grade 2 (99.9% Ti, Northwest Institute for Nonferrous Metal Research, Shanghai, China) was cut into 10-mm diameter sheets with a thickness of 1 mm. The sheets were carefully ground with Nos. 400, 600, 800, 1000, and 1200 SiC paper and were subsequently cleaned ultrasonically with pure acetone, ethanol and distilled water for 5 min.

The titanium sheets were divided into four groups: a control group, which consisted of the sheets processed using only the previously described steps, and three test groups classified according to the anodising voltage (Group 150 V, Group 180 V or Group 200 V). Anodic oxidation was performed at room temperature with a direct-current supply system (QUERLI DC power supply WYJ-500 V 1 A, China). A titanium sheet was used as the anode, and a titanium plate (20 mm × 20 mm × 1 mm) served as the cathode. A sodium acetate solution (1 mol/L) was used as the electrolyte, and three final voltages (150 V, 180 V and 200 V) were adopted to form a porous film on the titanium surface. The current density was 50 mA/cm^2, and the time at the final voltage was 2 min.

2.2. *Surface characterisation*

The surface microstructure, elemental composition and crystal structure of the titanium oxide films were observed using scanning electron microscopy (SEM, Hitachi, S-4800, Tokyo, Japan), energy dispersive X-ray spectroscopy (EDS, Hitachi, S-4800, Tokyo, Japan) and X-ray diffraction (XRD, X'Pert, PANalytical B.V., Almelo, Netherlands).

2.3. *Protein adsorption ability*

A bicinchoninic acid (BCA) protein assay (*20*) was adopted to measure the concentration of the proteins. Samples were placed in a 16-well cell culture plate. Approximately 1 mL of standard bovine serum albumin (BSA, 2 mg/mL) was added into each well, and the plate was placed on a thermostatic horizontal shaker for 2 h (50 rpm, 20°C). According to the Lambert-Beer law, the absorbance of a solution can be evaluated by its concentration at a given wavelength of light (*21*). Therefore, the optical density (OD) of the supernatant was measured at 562 nm using a spectrophotometer (TECAN SpectrofluorPlus); the concentration of the corresponding BSA solution was subsequently calculated, and the protein adsorption quantity of different surfaces was obtained.

2.4. *Antibacterial activity*

A modified antibacterial drop-test (*22*) was used to study the antibacterial activity of the samples. As the predominant bacterial flora in healthy peri-implant sulci, *Streptococcus mutans* (*23*) (*S. mutans*, ATCC 25175, provided by the State Key Laboratory of Oral Diseases, West China Hospital of Stomatology, Sichuan University) were chose and cultivated in brain-heart infusion (BHI) broth and anaerobically cultured (37°C, 80% N_2, 10% CO_2, 10% H_2) for 24 h. The bacteria-containing broth was centrifuged at 2,700 rpm for 10 min. The supernatant was discarded, and the bacteria were washed three times with phosphate-buffered saline (PBS). The bacteria were then resuspended in PBS at a concentration of 1×10^6 cfu/mL. All glassware and disk samples were sterilised with ultraviolet irradiation for 1 h beforehand. The bacterial suspension (1 mL) was added dropwise using a dispenser onto the surface of each sample in a 16-well plate, followed by incubation at 37°C for 24 h without stirring. After this period, the samples were washed three times with PBS and then resuspended in 4 mL PBS using ultrasonic vibration for 5 min at room temperature. The bacterial suspension was diluted 10,000-fold, and a 30-μL bacterial suspension of each sample was dropped onto the BHI solid medium to obtain a colony count after 48 h of incubation.

2.5. *L929 fibroblast adhesion*

L929 mouse fibroblasts (provided by the State Key Laboratory of Oral Diseases, West China Hospital of Stomatology, Sichuan University) were cultivated in Dulbecco's Modified Eagle Medium (DMEM) containing 10% foetal bovine serum (FBS) and 1% penicillin/streptomycin. An L929 fibroblast monolayer was formed, which was passaged upon confluence using trypsin (0.5% w/v in PBS). The cells were subsequently harvested from the culture by immersion in

trypsin solution for 5 min. The cells were centrifuged, and the supernatant was discarded. DMEM (3 mL) supplemented with serum was added to neutralise any residual trypsin, and then the cells were resuspended in serum-supplemented DMEM at a concentration of 1 × 10^4/mL. Afterward, the cells were cultivated in 5% CO_2 at 37°C.

The L929 cells were seeded onto different disk surfaces, and after a 24 h incubation, the sample surfaces were washed with PBS solution to remove loosely adsorbed cells. Cell fixation was performed with 4% glutaraldehyde in PBS for 4 h at 4°C, followed by dehydration with 25%, 50%, 70% and 95% (v/v) ethanol solutions for 15 min and final dehydration in absolute ethanol twice. The surfaces with immobilised cells were dried in supercritical carbon dioxide and were subsequently observed by SEM.

2.6. *Statistical analysis*

Statistical calculations were performed using the SPSS 17.0 software package. The differences were considered significant if the probability value was less than 5% ($p < 0.05$). SKEW and KURT tests were initially used to test the data for normality. A Levene test was conducted to examine the homogeneity of variance for multiple samples. Normally distributed data were expressed as the mean and standard deviation. For three-group comparisons, one-way ANOVA and Dunnett's *t*-test were used.

3. Results and Discussion

3.1. *Surface characterisation*

Figure 1 illustrates the surface SEM micrographs of the control samples and the samples anodised in 1M CH_3COONa for 2 min at different voltages. The surface of the control group showed scratches and grooves formed during mechanical grounding (Figure 1A). The surface processed by anodic oxidation at 150 V (Figure 1B) no longer showed visible scratches, and the surface consisted of randomly scattered pits and holes; diameters were approximately 100 nm to 3 μm. The surface subjected to an applied voltage of 180 V (Figure 1C) became uniform and was overlaid with densely distributed pores with sizes that ranged from 2 μm to 7 μm.The size of the pores did not change when the applied voltage was increased to 200 V (Figure 1D). Several larger-sized pores appeared, most likely because of the interconnection of some pores with each other (*24*). EDS analysis showed no contamination on any of the groups of disks (Figure 2).

Figure 3 shows the XRD patterns of the control group and the test groups. For the control group, only the peaks of titanium were observed. The XRD pattern of the surface treated with an applied voltage of 150 V indicated the presence of anatase phase, and the intensity of the anatase phase continued to increase until 180 V. The peaks of the rutile phase appeared in the pattern of the sample treated at 180 V, and the intensity of the corresponding peaks continued to increase as the anodisation voltage was increased from 180 V to 200 V, whereas the intensity of the peaks from the anatase phase and the titanium substrate decreased.

Starting with the growth of the amorphous TiO_2 (*25*), the formation of the anodic titanium oxides is

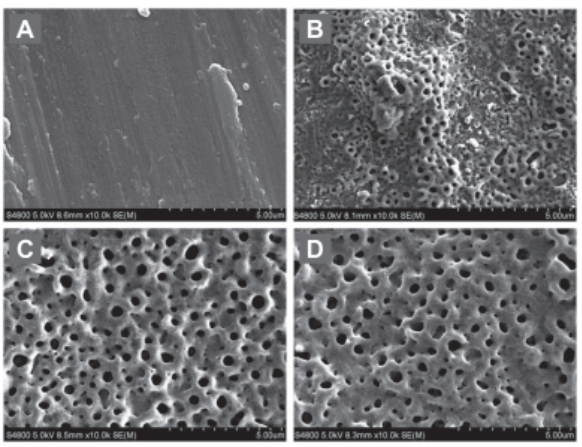

Figure 1. SEM images. (A) The control group, **(B)** Group 150 V, **(C)** Group 180 V and **(D)** Group 200 V.

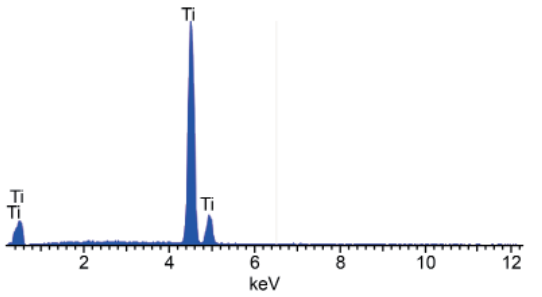

Figure 2. EDS graph of the anodic oxidation group.

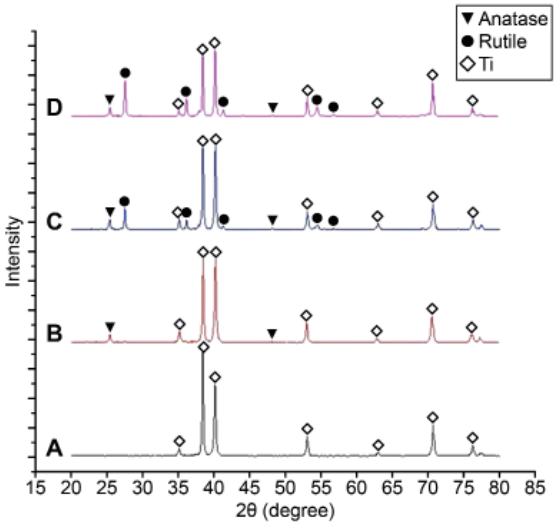

Figure 3. XRD graph. (A) The control group, **(B)** Group 150 V, **(C)** Group 180 V and **(D)** Group 200 V.

a process of competition between the deposition of the titanium oxides layer and the dissolution of that layer by the electrolyte (*26*). As the applied voltage is increased, the anodic oxidised film breaks down locally and porous regions become obvious because of the dielectric breakdown (*27*). According to our previous study (*25*), when the substrates were anodised in CH_3COONa electrolyte, spark discharges were observed on their surfaces beginning at ~135V; these discharges became more intense at higher anodising voltages. This behaviour accounts for the porous surface at 150 V observed by SEM. Meanwhile, spark discharges led to instantaneous, local high temperatures and pressures (*28*), so the initially produced amorphous titania was converted into the crystalline phases (*29*). The anatase structure was formed at the beginning and then transformed into the rutile phase with increasing voltage, which was consistent with the XRD results.

Among the three phases of titanium dioxide, rutile is known to be the most dense and stable phase and to exhibit the highest resistance to dissolution (*26*). As shown by the SEM results, the pore size and the porosity increased when the applied voltage was varied from 150 V to 180 V due to the growing field-assisted and chemical dissolution (*16*). However, as additional rutile formed during the crystallographic transformation, the dissolution resistance continued to increase, which led to similar pore sizes and porosities of the samples treated at 180 V and 200 V.

3.2. *Protein adsorption ability*

Figure 4 shows that the control sample exhibited presented the poorest adsorbing ability for proteins and that the protein adsorption ability increased as the applied voltage was increased from 150 V to 180 V. As the applied voltages increase, the thickness, surface roughness and porosity of the anodised TiO_2 layer increase (*27*), which, in turn, increase the biocompatibility and improve the protein adsorption ability (*26*). In addition, compared with rutile and amorphous titanium, anatase exhibits better bioactivity (*30,31*). Therefore, due to the decrease in the amount of anatase on the surface anodised at 200 V, the protein adsorption ability did not obviously change between Group 180 V and Group 200 V.

3.3. *Antibacterial activity*

The *S. mutans* colonies found on the culture were counted, and no significant difference in bacterial adherence was observed between the control group and Group 200 V or between Group 150 V and Group 180 V. The quantities of bacterial colonies observed in the control group and Group 200 V were much greater than those observed in Group 150 V and Group 180 V (Figure 5).

In the case of an applied voltage of 150 V, the increased antibacterial activity was attributed to the increase in the high photocatalytic crystalline phase of anatase (*22,32*). Although the amount of anatase structure continued to increase in samples treated up to 180 V, the appearance of the rutile phase, which decreases the photocatalytic activity of the TiO_2 film (*22*), made the antibacterial activity of the sample treated at 180 V almost the same as that treated at 150 V. In the case of the sample treated at an applied voltage of 200 V, in which the amounts of rutile and anatase increased and decreased, respectively, the antibacterial activity decreased sharply.

3.4. *L929 growth*

L929 fibroblasts were seeded onto the sample surface. After 24 h (*26*), some of the L929 fibroblasts started to develop pseudopods, and some fibroblasts spread out on the TiO_2 films, appearing in fusiform, polygonal and triangular shapes (Figure 6). As shown in the inset of Figure 6C, a single cell could be clearly observed to spread out its body and interlock to the porous surface with filopodia, whereas the cellular form and linkage were obscure in the control group. Furthermore, the cell concentration on the uncoated titanium surface was obviously lower than on the other surfaces, and the cell concentrations on the titanium surfaces anodised at 180 V and 200 V stood out, which can be attributed to the enhanced biological performance of the anodised TiO_2 surfaces (*33*).

It's widely accepted that application of the porous

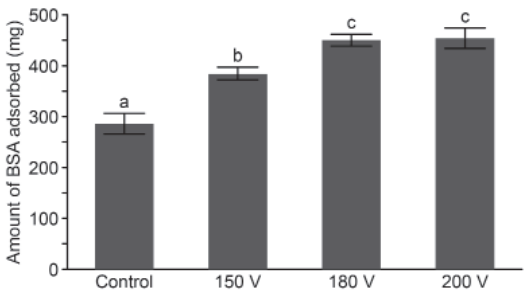

Figure 4. Amount of bovine serum albumin (BSA) adsorbed onto different surfaces. (a, b, c) Different letters indicate a significant difference at $p < 0.05$.

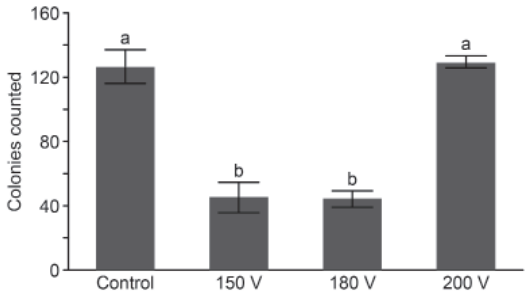

Figure 5. Number of *Streptococcus mutans* colonies that adhered to the different surfaces. (a, b) Different letters indicate a significant difference at $p < 0.05$.

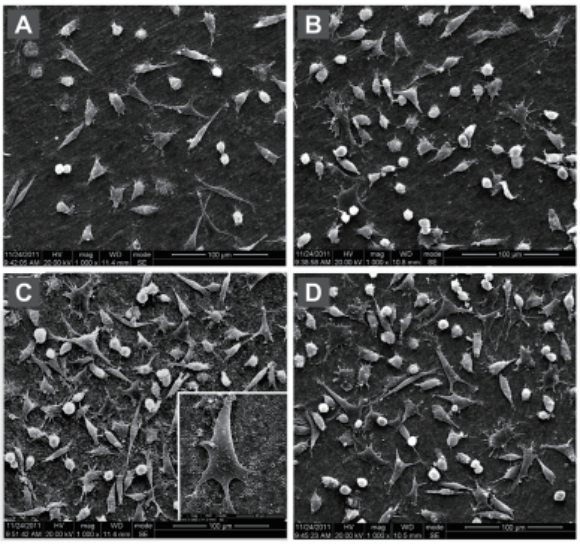

Figure 6. SEM images of L929 cells cultured for 24 h on different surfaces. (A) The control group, **(B)** Group 150 V, **(C)** Group 180 V and **(D)** Group 200 V. The cell concentrations on the titanium surfaces anodised at 180V (C) and 200V (D) stood out, which indicates better cell adhesion and proliferation. The inset shows a higher-magnification image in which a single cell could be clearly observed to spread out its body and interlock to the porous surface with filopodia.

surface can greatly improve the outcome of cell seeding (*34*), just in accordance with the significant higher cell concentration on the titanium surfaces of the test groups. Squier *et al*. (*8*), on the basis of an *in vitro* study, suggested that 3 μm is the minimum pore size that permits penetration of the connective tissue, thus, the collagen fibres are oriented perpendicularly to the implant surface and epithelial downgrowth is markedly restricted when the pore sizes are larger than 3 μm. Therefore, we determined that a greater cell concentration results in a fully spread-out morphology and that the obvious anchorage on the titanium surfaces anodised at 180 V or 200 V may be the result of the adequate pore sizes formed at these voltages. In addition, as the protein adsorption ability of the materials acts as the base to support cell adhesion and proliferation (*26*), the bacterial adhesion performances were consistent with the protein adsorption results.

4. Conclusion

The porous TiO_2 films formed through anodisation at 180 V promote the adsorption of proteins, inhibit bacterial adhesion and enhance fibroblast growth, which indicates that anodisation positively affects biological seal formation in the neck region.

Acknowledgements

This work was supported by the National Natural Science Foundation of China (Project No. 81070868/H1409). We acknowledge the staff and faculty at the State Key Laboratory of Oral Diseases, Sichuan University for their assistance.

References

1. Buser D, Belser UC, Lang NP. The original one-stage dental implant system and its clinical application. Periodontol. 2000 1998; 17:106-118.
2. Sul YT, Jeong Y, Johansson C, Albrektsson T. Oxidized, bioactive implants are rapidly and strongly integrated in bone. Part 1--experimental implants. Clin Oral Implants Res. 2006; 17:521-526.
3. Holt RL, Rosenberg MM, Zinser PJ, Ganeles J. A concept for a biologically derived, parabolic implant design. Int J Periodontics Restorative Dent. 2002; 22:473-481.
4. Schupbach P and Glauser R. The defense architecture of the human periimplant mucosa: A histological study. J Prosthet Dent. 2007; 97:S15-25.
5. Glauser R, Schupbach P, Gottlow J, Hammerle CH. Periimplant soft tissue barrier at experimental one-piece mini-implants with different surface topography in humans: A light-microscopic overview and histometric analysis. Clin Implant Dent Relat Res. 2005; 7(Suppl 1):S44-51.
6. Comut AA, Weber HP, Shortkroff S, Cui FZ, Spector M. Connective tissue orientation around dental implants in a canine model. Clin Oral Implants Res. 2001; 12:433-440.
7. Tete S, Mastrangelo F, Bianchi A, Zizzari V, Scarano A. Collagen fiber orientation around machined titanium and zirconia dental implant necks: An animal study. Int J Oral Maxillofac Implants. 2009; 24:52-58.
8. Squier CA and Collins P. The relationship between soft tissue attachment, epithelial downgrowth and surface porosity. J Periodontal Res. 1981; 16:434-440.
9. Oh TJ, Yoon J, Misch CE, Wang HL. The causes of early implant bone loss: Myth or science? J Periodontol. 2002; 73:322-333.
10. Rutar A, Lang NP, Buser D, Burgin W, Mombelli A. Retrospective assessment of clinical and microbiological factors affecting periimplant tissue conditions. Clin Oral Implants Res. 2001; 12:189-195.
11. Bratu EA, Tandlich M and Shapira L. A rough surface implant neck with microthreads reduces the amount of marginal bone loss: A prospective clinical study. Clin Oral Implants Res. 2009; 20:827-832.
12. Simion M, Baldoni M and Rossi P. A study on the attachment of human gingival cell structures to oral implant materials. Int J Prosthodont. 1991; 4:543-547.
13. Mustafa K, Oden A, Wennerberg A, Hultenby K, Arvidson K. The influence of surface topography of ceramic abutments on the attachment and proliferation of human oral fibroblasts. Biomaterials. 2005; 26:373-381.
14. Ishizawa H and Ogino M. Characterization of thin hydroxyapatite layers formed on anodic titanium oxide films containing Ca and P by hydrothermal treatment. J Biomed Mater Res. 1995; 29:1071-1079.
15. Kim HM, Miyaji F, Kokubo T, Nishiguchi S, Nakamura T. Graded surface structure of bioactive titanium prepared by chemical treatment. J Biomed Mater Res. 1999; 45:100-107.
16. Park IS, Lee MH, Bae TS, Seol KW. Effects of anodic oxidation parameters on a modified titanium surface. J

Biomed Mater Res B Appl Biomater. 2008; 84:422-429.
17. Zhu X, Kim KH, Jeong Y. Anodic oxide films containing Ca and P of titanium biomaterial. Biomaterials. 2001; 22:2199-2206.
18. Ishizawa H, Ogino M. Formation and characterization of anodic titanium oxide films containing Ca and P. J Biomed Mater Res. 1995; 29:65-72.
19. Sul YT, Johansson CB, Jeong Y, Albrektsson T. The electrochemical oxide growth behaviour on titanium in acid and alkaline electrolytes. Med Eng Phys. 2001; 23:329-346.
20. Smith PK, Krohn RI, Hermanson GT, Mallia AK, Gartner FH, Provenzano MD, Fujimoto EK, Goeke NM, Olson BJ, Klenk DC. Measurement of protein using bicinchoninic acid. AnalBiochem. 1985; 150:76-85.
21. Gao L, Feng B, Wang J, Lu X, Liu D, Qu S, Weng J. Micro/nanostructural porous surface on titanium and bioactivity. J Biomed Mater Res B Appl Biomater. 2009; 89:335-341.
22. Trapalis CC, Keivanidis P, Kordas G, Zaharescu M, Crisan M, Szatvanyi A, Gartner M. TiO2(Fe3+) nanostructured thin films with antibacterial properties. Thin Solid Films. 2003; 433:186-190.
23. Kocar M, Seme K, Hren NI. Characterization of the normal bacterial flora in peri-implant sulci of partially and completely edentulous patients. Int J Oral Maxillofac Implants 2010; 25:690-8.
24. Sul YT, Johansson CB, Petronis S, Krozer A, Jeong Y, Wennerberg A, Albrektsson T. Characteristics of the surface oxides on turned and electrochemically oxidized pure titanium implants up to dielectric breakdown: The oxide thickness, micropore configurations, surface roughness, crystal structure and chemical composition. Biomaterials. 2002; 23:491-501.
25. Xie L, Liao XM, Xu H, Yin GF, Huang ZB, Yao YD, Chen XC, Gu JW. A facile one-step anodization treatment to prepare multi-level porous titania layer on titanium. Mater Lett. 2012; 72:141-144.
26. Xie L, Yin G, Yan D, Liao X, Huang Z, Yao Y, Kang Y, Liu Y. Structure, morphology and fibroblasts adhesion of surface-porous titanium *via* anodic oxidation. J Mater Sci Mater Med. 2010; 21:259-266.
27. Kuromoto NK, Simao RA, Soares GA. Titanium oxide films produced on commercially pure titanium by anodic oxidation with different voltages. Mater Charact. 2007; 58:114-121.
28. Wu HH, Lu XY, Long BH, Wang XQ, Wang JB, Jin ZS. The effects of cathodic and anodic voltages on the characteristics of porous nanocrystalline titania coatings fabricated by microarc oxidation. Mater Lett. 2005; 59:370-375.
29. Li LH, Kong YM, Kim HW, Kim YW, Kim HE, Heo SJ, Koak JY. Improved biological performance of Ti implants due to surface modification by micro-arc oxidation. Biomaterials. 2004; 25:2867-2875.
30. Yang TS, Shiu CB, Wong MS. Structure and hydrophilicity of titanium oxide films prepared by electron beam evaporation. Surf Sci. 2004; 548:75-82.
31. Sun LC, Hou P. Spectroscopic ellipsometry study on e-beam deposited titanium dioxide films. Thin Solid Films. 2004; 455:525-529.
32. Zhang HJ, Wen DZ. Antibacterial properties of Sb-TiO_2 thin films by RF magnetron co-sputtering. Surf Coat Technol. 2007; 201:5720-5723.
33. Sul YT, Johansson CB, Jeong Y, Roser K, Wennerberg A, Albrektsson T. Oxidized implants and their influence on the bone response. J Mater SciMater Med. 2001; 12:1025-1031.
34. Dai W, Dong J, Chen G, Uemura T. Application of low-pressure cell seeding system in tissue engineering. Biosci Trends. 2009; 3:216-219.

(Received March 2, 2014; Revised August 10, 2014; Re-revised October 9, 2014; Accepted October 10, 2014)